Synchronization, attractor fission, and attractor fusion in a globally coupled laser system

Kenju Otsuka and Jyh-Long Chern
NTT Basic Research Laboratories, Nippon Telegraph and Telepone Corporation, Musashino-shi, Tokyo 180, Japan
(Received 8 July 1991)

A globally coupled class-*B* laser array with incoherent feedback is proposed for exploring the complex dynamics of dynamical systems with the highest connectivity. This feedback shows a fundamental characteristic, *information lag*, and results in the general features of synchronization, attractor fission, and attractor fusion processes. The common characteristics shared by different clusters in the segregation process are found. The effect of multiple different time delays on synchronization is also investigated.

PACS number(s): 42.60.Da, 42.50.Fx, 42.50.Lc, 42.60.Fc

Complex dynamics in high-dimensional nonlinear systems is a current issue of interest in various physical systems. The fundamental issue is how self-organization can be established from the interacting elements. For a well-organized biological system, e.g., the brain, connectivity among elements is high [1]. This is our basic motivation for studying the complex dynamics of high-connectivity systems. The highest connectivity occurs in global coupling (GC), in which every element is coupled with every other element. Needless to say, delays are inevitable in such a system but delay in coupled-element systems is still an open subject.

In the meantime, recent progress in limit-cycle oscillators [2] and GC dynamical systems, such as coupled mapping lattices (GCM) [3], Josephson junction arrays [4], and multimode lasers [5], have stimulated great interest in, for example, the understanding of synchronization and memories of huge capacity based on antiphase states and clusters. Clusters seem to be a universal feature of globally coupled systems. An open question is: *What characteristics are shared by different clusters?* Also, because of high-speed processing, it is worthwhile to consider the possibility of high connectivity in an all-optical system.

In modern optics, Ikeda initiated delay-induced complex phenomena and predicted period-doubling bifurcation leading to chaos in a bistable *one-element* ring cavity and frustrated instability in a Fabry-Pérot resonator [6]. The feedback effect also results in chaos in lasers. Another example is charotic behavior in semiconductor lasers with coherent external feedback [7]. Instabilities and Shil'nikov chaos have been demonstrated in a CO_2 laser with nonlinear electronic feedback [8]. On the contrary, for a coupled-element system with multiple different time delays an intriguing question is: *Does synchronization occur?* In this article, we propose a simple scheme, a laser with GC delayed incoherent feedback (LDIF), as a promising candidate for answering the above two questions.

In our model, class-B laser elements are arranged to form a GC laser array. These elements interact via a multiport fiber or beam splitter by means of incoherent feedback. All-optical incoherent feedback employing polarization rotation [9] is also applicable to linearly polarized lasers. The incoherent coupling is introduced so as to be able to neglect the phase dynamics and coherent feedback, and the incoherent feedback beam directly modulates the population inversion only with delay, i.e., *information lag*. Therefore the dynamics are described by the coupled difference-differential equations,

$$\frac{dn_k(t)}{dt}=w-n_k(t)\left[1+s_k(t)+\frac{\gamma}{N}\sum_{j=1}^{N}(t-T_{k,j})\right], \tag{1}$$

$$\frac{ds_k(t)}{dt}=K\{[n_k(t)-1]s_k(t)+\epsilon_k n_k(t)\}, \quad k=1,2,\ldots,N, \tag{2}$$

where t has been rescaled with the population lifetime τ, $K\equiv\tau/\tau_p$, and τ_p is the photon lifetime. The terms w, n_k, s_k, and ϵ_k are, respectively, the normalized pump power, population-inversion density, photon density, and the spontaneous-emission coefficient of the kth laser element. γ indicates the coupling strength, $T_{k,j}=(L_{k,j}/c)/\tau$ in which $L_{k,j}$ is the optical path of feedback from elements j to k, c is the velocity of light, and N is the total number of laser elements in the array [10].

First, let us assume the simplest case, $T_{k,j}=T$ for all k and j. The steady states $\hat{n}_k$ and $\hat{s}_k$ of Eqs. (1) and (2) are determined by

$$\hat{n}_k\approx 1, \quad \hat{s}_k=\frac{w-1}{1+\gamma}, \tag{3}$$

assuming $\epsilon w \ll 1$ ($\epsilon_k=\epsilon$ for all k). There are other steady states with one or several $\hat{s}_k=0$, which are unstable. The linear stability analysis (LSA) is performed by assuming $x=\hat{x}+\delta x$ and $\delta x=\delta\hat{x}e^{\lambda t}$ ($x=n_k$ or s_k) in Eqs. (1) and (2) with (3). The characteristic equation follows

$$\lambda^2+w\lambda+\frac{K(w-1)}{1+\gamma}\gamma e^{i2l\pi/N}e^{-\lambda T}+\frac{K(w-1)}{1+\gamma}=0, \tag{4}$$

where $l=0,1,2,\ldots,N-1$. Similar to Ref. [11], the linear stability is determined by $l=0$ only as that of the (0,0) mode of Ref. [11]. With an increase in w, the system can show a self-sustained relaxation oscillation ω_{RO} via Hopf bifurcation at $w=w_{th,2}$. We solve [12] Eq. (4) with $l=0$ to determine the stable regime, $\mathrm{Re}(\lambda)<0$ for all λ. As shown in Fig. 1, there are two thresholds, the $w_{th,2}$ of the lower branch and the $w_{th,3}$ of the upper branch. For $w<w_{th,2}$ or $w>w_{th,3}$, only damping oscillation can be found. Unstable motion arises when $w_{th,2}<w<w_{th,3}$, which has been numerically confirmed. This stability diagram is universally valid and independent of N.

Let us consider the dynamics in unstable regimes, which depend on the system size N. The state change for $N=5$ is depicted in Fig. 1 for $T=0.03$ and $\gamma=0.21$. A series of output wave forms and corresponding phase-space trajectories (n_k,s_k) for different w in an unstable regime are shown in Fig. 2. As soon as w exceeds $w_{th,2}$, the damping oscillation is replaced by a self-sustained oscillation whose frequency coincides with the analytical results. This self-pulsation is induced by delay. Because of the feedback loop, the damping oscillation is continuously memorized and fed back to the system. This acts as a successive-pulse modulation on the system. If the delay is not too long, then the laser will be driven by this modulation to produce a modulated output. This output is again fed back to the system and the return beam perturbs the population inversion further. If such a positive-feedback modulation balances with the damping force of the relaxation oscillation, the system evolves itself to a state of sustained relaxation oscillation, as shown in Fig. 2(a) and 2(a'). When w is increased, quasiperiodic relaxation oscillations appear through increased perturbation around ω_{RO}. This is the physical mechanism of self-pulsation in this system, which is totally different from those of Refs. [6–8]. When γ is increased, the

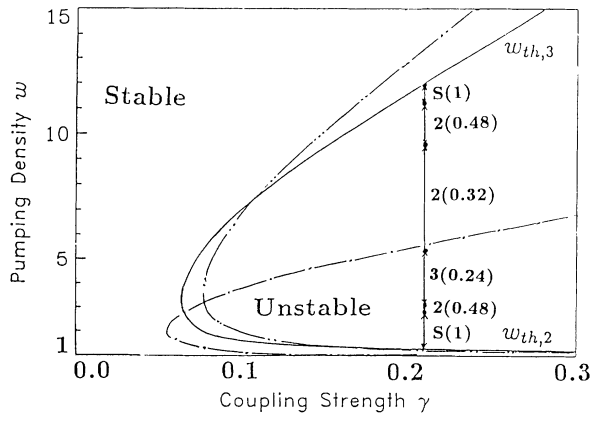

FIG. 1. Stability diagram where stability boundaries are for the quotes "—" line, $T=0.03$, $K=1000$; "—●—" line, $T=0.05$, $K=1000$; and "—●●—" line, $T=0.03$, $K=800$. In the unstable regime, a typical attractor fission and fusion process is shown with $\gamma=0.21$, $\epsilon=1.2\times10^{-7}$, where S is the synchronized state, 2 is the two-cluster state, 3 is the three-cluster state. The numbers in parentheses are the probabilities of two different elements being within the same cluster.

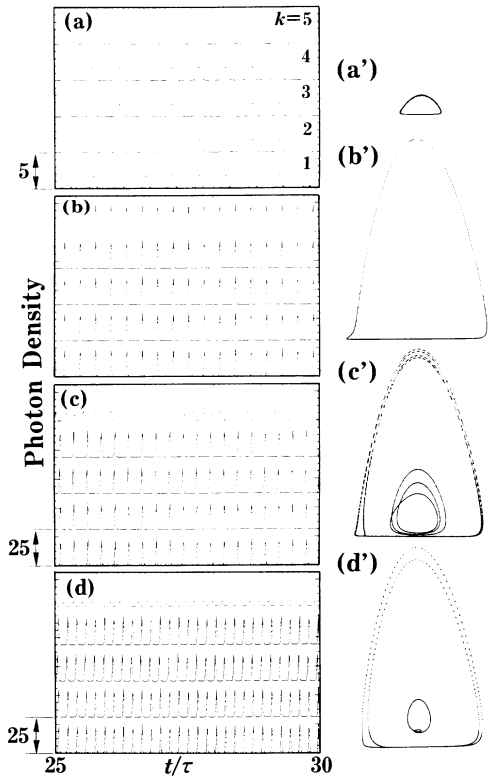

FIG. 2. Time series (a)–(d) and (n_k,s_k) projection of phase space (a')–(d') for different w assuming $\gamma=0.21$, $T=0.03$, $K=1000$, $\epsilon=1.2\times10^{-7}$. (a) and (a'), $w=1.3$; (b) and (b'), $w=2.7$; (c) and (c'), $w=2.9$; and (d) and (d'), $w=4.0$.

modulation depth will be increased due to the increase in feedback light intensity. This results in a lower $w_{th,2}$ for a larger γ, as shown in Fig. 1. Also, larger K and T result in lower $w_{th,2}$.

The self-sustained oscillations near the boundary $w_{th,2}$ are synchronized as shown in Fig. 2(a). Many random initial values were used to test the synchronization and it was found that this synchronization state corresponds to the creation of a single attractor in the phase space. Let us provide a physical interpretation for synchronization. Suppose there are small inhomogeneous (k-dependent) deviations from $\hat{n}_k$ and $\hat{s}_k$. From Eq. (1) the site dependence of n_k is negligible if the feedback photon number $(\gamma/N)\sum_{j=1}^{N}s_j$ is small. Therefore, all n_k are perturbed in the same fashion by this number, i.e., GC, and all s_k are synchronized through Eq. (2). [See Figs. 2(a) and 2(b).] When N is increased, feedback intensity $(\gamma/N)\sum_{j=1}^{N}s_j$ increases and the perturbation becomes strong, exceeding the LSA regime. At this moment, the initial small inhomogeneity in n_k is enlarged by the strong perturbation based on Eq. (1). As a consequence, the population dynamics become site dependent and synchronization fails. We also simulated the case of unequal pumping. Even in this case, if the coupling strength is larger than the pumping fluctuation or one-site nonlinearity, the system exhibits synchronization or quasisynchronization.

As soon as synchronization disappears, segregation of

motion takes place among laser elements as shown in Figs. 2(c) and 2(d). *Attractor fission,* which means the self-induced breakup of a global attractor (synchronized motion), is used to describe this process. A similar phenomenon has been referred to as cluster forming in GCM [2]. Avoiding excessive complexity, we investigate the segregation process in our system with $N=5$. It is found that as w increases, the elements separate one by one from the synchronization state and form clusters (segregation). Because of linear feedback, increasing w means increasing only the depth of modulation as mentioned before. This drives the system to a quasiperiodic or even chaotic orbit. It is found in the present parameter regime that before the onset of the segregation process, a quasiperiodic orbit is created in the synchronization state [see Fig. 2(b)]. Then one of the elements (e.g., $k=5$) separates from this synchronized state, as shown in Fig. 2(c).

The frequency components embedded in the quasiperiodic orbit are expected to provide the key to understanding segregation. Therefore, we carried out a power-spectrum (PS) analysis. The PS's which correspond to Fig. 2 are shown in Fig. 3. In the transition process from synchronized quasiperiodic motion [Fig. 2(b)] to the segregated state [Fig. 2(c)], the $k=1,2,4,3$ elements follow the nature of Fig. 2(b) with an enhanced quasiperiodicity. To be more specific, the $k=1,2,3,4$ elements are synchronized at $w=27.5$ (two-cluster state), while the $k=3$ element becomes slightly different at $w=27.9$, although their spectra are almost the same. During this process, the $k=5$ element is segregated. Its dynamics are determined so as to satisfy the constraint condition of $\langle \sum_{j=1}^{N} s_j \rangle_{\text{long time average}} = N(w-1)/(1+\gamma)$, and the system forms a three-cluster state at $w=2.9$. It is noticed that inhomogeneity of $\langle s_k \rangle_{\text{long time average}}$ among the clusters occurs. We note that the ratio of the dominant frequencies of $k=5$ and the other clusters maintain $f_1/f_1=\frac{2}{3}$ and such a locking state among clusters exists in a wide w region up to $w=3.5$. Unlike GCM [3] there coexist at least $N!/N_1!N_2!\ldots N_k!$ orbits in such a k-cluster state, where N_k is the element number in the kth cluster. Increasing w results in larger modulation depth and enhances the GC strength; thus the system tends to be locked at the least common frequency components above ω_{RO} of all clusters and therefore the system evolves to a three-cluster state with the same fundamental frequency f_3, as shown in Figs. 2(d) and 3(d) and 3(d').

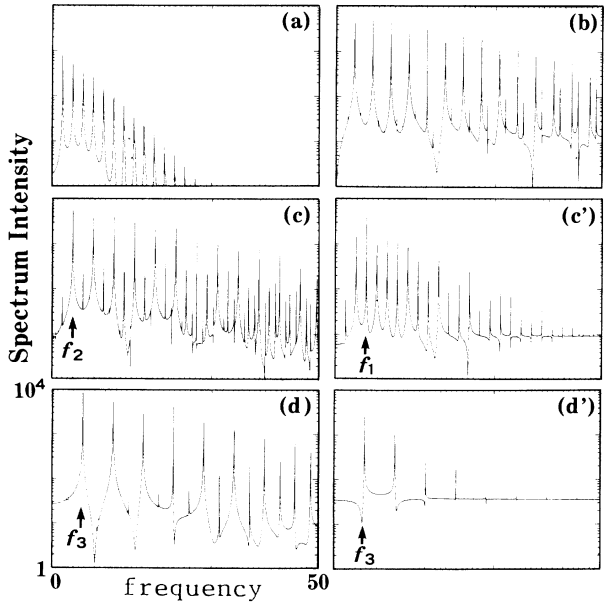

FIG. 3. Corresponding fast-Fourier-transform (FFT) spectra for Fig. (2). (c') and (d') $k=5$.

As w increases further, the inverse process takes place. This process, *attractor fusion,* corresponds to the unification of all the coexisting attractors, and it leads to a stable state above $w_{\text{th},3}$. A higher pumping drives the system to a stable state as shown in Fig. 1. We noted that the self-pulsation found in the present system is a type of self-sustained oscillation, and it originates from the relaxation oscillation and successive-feedback modulation. LSA indicates that higher pumping results in a higher damping rate. If the damping force is strong enough, feedback-induced modulation is damped out, and no sustained oscillation can be established. In the case of large T, its characteristic information lag is essential and results in the blackout of memory of past system evolution.

Next let us consider the effects of multiple *different* time delays, which are expected in real systems, on synchronization. Because of different delays, feedback beams trigger each element differently. The underlying self-organization mechanisms are quite intricate. We approach this issue by extensive numerical simulation [13]. For comparison, we first simulate the case of $T_{k,j}=T_k$ for all j. In Fig. 4 the average of different randomly chosen time delays versus the standard deviation is shown for $w=2$ of $N=7$. Hundreds of data are plotted; the square, star, and triangle symbols mean the cluster state, synchronization, and steady state, respectively. The data can be roughly classified into five regimes. In

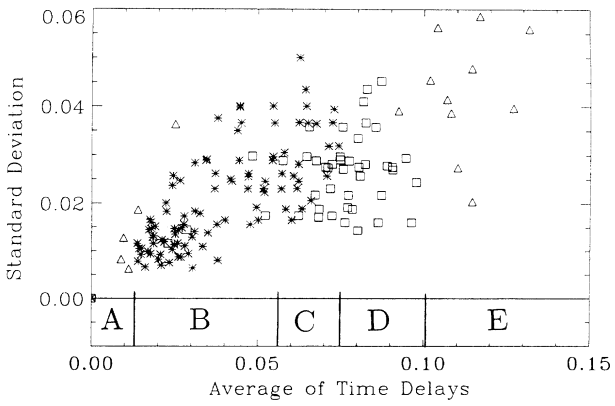

FIG. 4. The average of randomly chosen time delays vs the standard deviation for $w=2$ of $N=7$, where $\gamma=0.21$, $k=1000$, and $\epsilon=1.2\times10^{-7}$. The symbols square, star, and triangle mean the cluster state, synchronization state, and steady state, respectively.

regime A, only the steady state appears. It is found that in regime B, the system has a great probability of achieving synchronization, which results from an adequate *firing on time* among the feedback beams in the case of small decays. Synchronization and clustering are mixed with almost equal probabilities in regime C. Regime D is mostly occupied by cluster states. In regime E only the steady state appears. The existence of regimes A and E indicates the process of attractor fission and fusion and shows again the fundamental characteristic of incoherent feedback. For the case of arbitrary $T_{k,j}$, wave forms are very complicated. It is surprising to note that synchronization is replaced by a frequency locking among elements with a fixed phase difference of the order of (0.01 sec)/τ in the case of small average delay. Again the process of attractor fission and fusion resulting from incoherent feedback is found.

In summary, a simple scheme for exploring the dynamical systems of high connectivity is proposed. In the GC case, the clustering process is triggered by the appearance of a quasiperiodic orbit in which new frequency components are embedded. This attractor fission is established by delay, which acts fundamentally as information lag. This simple characteristic is very general, and it is also the origin of the attractor-fusion process. A dominant-frequency locking among different clusters is found; this is a common characteristic shared by different clusters in the segregation process. Synchronization with multiple different time delays is found numerically. More analytical approaches are needed, e.g., to determine the boundaries of the different regimes in Fig. 4. We hope that this work will stimulate investigation on the effects induced by multiple time delays in coupled-element systems.

[1] J. Hertz, A. Krogh, and R. G. Palmer, *Introduction to the Theory of Neural Computation* (Addison Wesley, New York, 1991).

[2] P. C. Matthews and S. H. Strogatz, Phys. Rev. Lett. **65**, 1701 (1990); S. H. Strogatz, C. M. Marcus, R. M. Westervelt, and R. E. Mirollo, Physica D **36**, 23 (1989).

[3] K. Kaneko, Phys. Rev. Lett. **63**, 219 (1989); Physica D **41**, 137 (1990).

[4] P. Hadley and M. R. Beasley, Appl. Phys. Lett. **50**, 621 (1987).

[5] G. E. James, E. M. Harrell, II, and R. Roy, Phys. Rev. A **41**, 2778 (1990); K. Wiesenfeld, C. Bracikowski, G. James, and R. Roy, Phys. Rev. Lett. **65**, 1749 (1990); K. Otsuka, *ibid.* **67**, 1090 (1991).

[6] K. Ikeda, H. Daido, and O. Akimoto, Phys. Rev. Lett. **45**, 709 (1980); K. Ikeda and M. Mizuno, *ibid.* **53**, 1340 (1984).

[7] T. Mukai and K. Otsuka, Phys. Rev. Lett. **55**, 1711 (1985); J. Mørk, J. Mark, and B. Tromborg, *ibid.* **65**, 1999 (1990).

[8] F. T. Arecchi, R. Meucci, and W. Gadomski, Phys. Rev. Lett. **58**, 2205 (1987); F. T. Arecchi, W. Gadomski, A. Lapucci, H. Mancini, R. Meucci, and J. A. Roversi, J. Opt. Soc. Am. B **5**, 1153 (1988).

[9] H. Yasaka and H. Kawaguchi, Appl. Phys. Lett. **53**, 1360 (1988). If a Fabry-Pérot étalon is replaced by a mirror, LDIF is attained.

[10] K. Otsuka, IEEE J. Quantum Electron. **QE-15**, 655 (1979).

[11] J.-L. Chern, J. K. McIver, and J.-T. Shy, Opt. Commun. **76**, 63 (1990).

[12] S. J. Bhatt and C. S. Hsu, J. Appl. Mech. **33**, 113 (1966).

[13] Our code is adapted from E. Hairer, S. P. Norsett, and G. Wanner, *Solving Ordinary Differential Equation I: Nonstiff Problems* (Springer-Verlag, Berlin, 1987), pp. 286–300. We also verified our code with some analytical works of multiple time delays, e.g., W. Huang, J. Math. Anal. Appl. **148**, 360 (1990).